

BEAM ALIGNMENT STRATEGY AT THE BEAM TRANSPORT LINE FOR J-PARC MUON g-2/EDM EXPERIMENT*

H. Iinuma[†], M. Kusuba, H. Sato, Ibaraki-University, Mito, Japan
H. Nakayama, S. Ogawa, M. Otani, K. Sasaki, M. Abe, T. Mibe, KEK, Tsukuba, Japan
R. Matsushita, T. Sato, University of Tokyo, Tokyo, Japan

Abstract

To realize very precise measurement of the muon spin precession frequency in the level of sub-ppm, a muon beam is injected into a precisely adjusted storage magnet of sub-ppm uniformity via “Three-dimensional spiral beam injection scheme” at J-PARC muon g-2/EDM experiment. This injection scheme requires a strongly X-Y coupled beam which is applied by seven rotating quadrupoles on the upstream beam transport line. In this presentation, requirement and strategy for precise control of the X-Y coupling at the beam transport line and beam channel in the yoke of the storage magnet are discussed.

MOTIVATION

A new experiment planned at J-PARC [1] aims a different approach to those of previous muon g-2 experiments. In a departure from the so-called magic momentum $\gamma = 29.3$, a low-momentum ($\gamma = 3$) with small emittance muon beam allow us to maintain the muon beam in the storage ring by use of only weak magnetic focusing. An unit of 3 T MRI-type solenoid magnet will be used to store such new muon beam. The diameter of the orbital cyclotron motion becomes only 0.66 m, which is a factor of 20 smaller than that of the former experiments.

This small storage ring allow us to explore muon electric dipole moment (EDM), as well as g-2, although the conventional two-dimensional injection scheme is not applicable for such small ring. To achieve sensitivity of order $d_\mu \sim 10^{-21} e \cdot \text{cm}$, target value of vertical size of the storage beam is required to be less than 0.05 m. This newly developed three-dimensional injection scheme [2] allows for precise beam control of the storage plane in such a compact ring.

OUTLINE OF THREE-DIMENSIONAL SPIRAL BEAM TRAJECTORY

Figure 1 depicts outline of three-dimensional injection trajectory and storage magnet. The beam enters the solenoid through a channel in the top iron yoke 1.1 m above the storage volume and its spiral motion is compressed by the Fleming force owing to the static radial field. A vertical kick (pulsed radial magnetic field) is applied to store the beam on arrival to the storage region. A small static weak-focusing field in the fiducial volume maintains the beam in the storage region.

* Work supported by JPS KAKENHI Grant Numbers JP19H00673 and JP20H05625.

[†] hiromi.iinuma.spin@vc.ibaraki.ac.jp

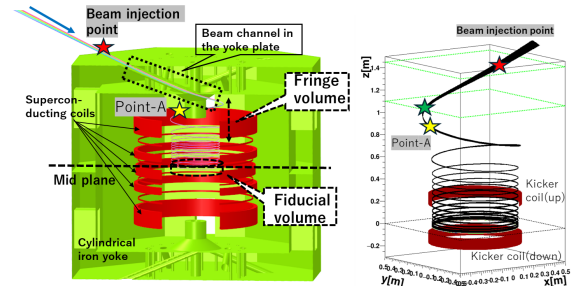


Figure 1: Storage magnet and beam injection.

Design of a reference orbit comes first, then parameters of the vertical kicker are designed as in [3]. Because of a finite emittance of the incoming muon beam, not all the muons do not get stored as the reference orbit. To maximize the injection efficiency, a dedicated beam control is employed in the three-dimensional spiral injection. A design of those beam control is discussed in the next.

REQUIRED PHASE SPACES

Beam Shape Inside of the Yoke

Figure 2 depicts phase space at $z=0.95$ m on the beam coordinate: $x-x'$, $y-y'$, $x-y$, x^2-y^2 , x^2-y and $y-x'$ for two cases. The pink colored distribution is ideally correlated in six ways plots which are adjusted with spatial distribution of fringe field of $0.6 < z < 0.95$ m [2]. We call this as type-A. The other in black colored distribution has no phase space correlation. We call this type-B.

Left side of Figure 3 depicts vertical phase space $z(t)-z'(t)$ during the kick period for type-A and type-B. Although the same kicker parameter is applied for both, it is obvious that type-A is better controlled in vertical dispersion. Right side of Figure 4 depicts a time slice of vertical correlation at the end of the kick: $z-z'$. Two blue ellipses are eye-guide of vertical betatron oscillation (VBO) in the weak focusing field for VBO amplitude 50 mm and 100 mm. Each beam particle satisfies within the ellipse at the end of the kick can stay inside the ellipse during the storage. Outline shape of $z-z'$ time-slice is come from a kicker coils' shape. However, a distributions along the $z-z'$ time-slices are different among type-A and type-B, as in left plot of Fig. 4.

In this paper, We define injection efficiency as the ratio of the number of the particle inside the VBO < 50 mm out of all injected particles, 80% for type-A and 20% for type-B.

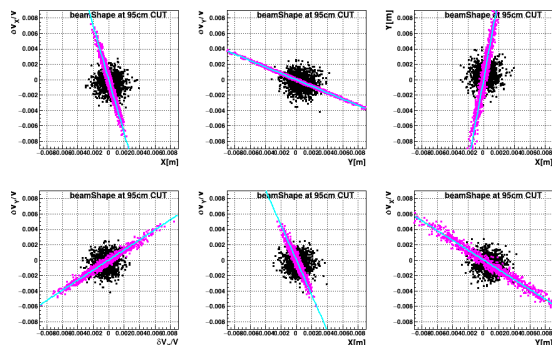


Figure 2: Phase space at $z=0.95$ m as pointed with yellow star in Fig. 1. The pink colored distribution called type-A is ideally correlated. Black colored distribution called type-B has no phase space correlation. Aqua-blue solid lines are linear fit of pink colored distributions.

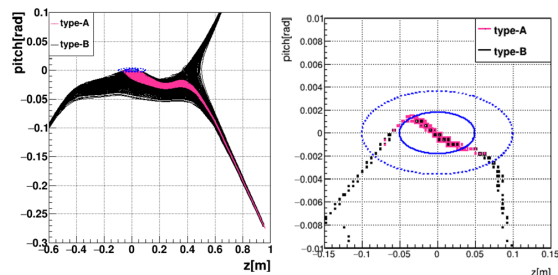


Figure 3: Left: Vertical phase space during the kick for both types A and B. Starting from initial position around $z=0.95$ m to stored volume center of $z=0$ m. Right: vertical phase space just at end of the kick.

One of the way of a method for evaluating how well the current phase space matches a specific X-Y coupling is using five parameters as Eq. (1) in the lab from which is discussed details in [3]. A particle in the storage magnet system coordinate is expressed as:

$$\vec{r} = (x, y, z), \vec{p} = (p_x, p_y, p_z). \quad (1)$$

By use of three angles:

$$\phi = \cos^{-1} \frac{x}{\sqrt{x^2 + y^2}}, \quad \psi = \cos^{-1} \frac{p_x}{\sqrt{p_x^2 + p_y^2}}, \quad (2)$$

$$\theta = \sin^{-1} \frac{p_z}{|p|},$$

we define five-components vectors of particle i^{th} ;

$$\vec{q}_i = (|r_i|, z_i, \phi_i, \theta_i, \psi_i), \quad \delta \vec{q}_i = \vec{q}_i - \vec{q}_g. \quad (3)$$

Subscript 0, 1, ..n is each particle identification number and g denotes beam center.

Inner product of the smallest singular value decomposition vector \vec{s} of $\mathcal{M}_{tot} = (\delta \vec{q}_0^T, \dots, \delta \vec{q}_n^T)$ and \vec{q}_i

$$d_i = \vec{s} \cdot \vec{q}_i \quad (4)$$

for each particle has distribution as in right side of Fig. 4. Comparing left and right plots of Fig. 4 confirms that particle which satisfies $VBO < 0.5$ m also satisfies small value of Eq. (4).

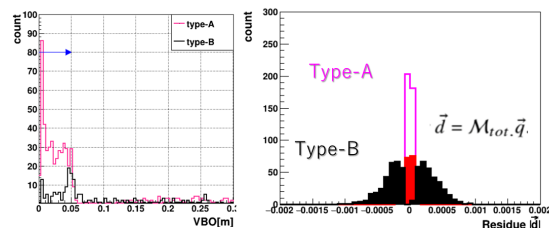


Figure 4: Left: Vertical phase space during the kick for both types A and B. Starting from initial position around $z=0.95$ m to stored volume center of $z=0$ m. Right: vertical phase space just at end of the kick.

Magnetic Field in the Channel of the Yoke

Beam is injected via channel in the yoke. The channel is cylindrical shape with diameter 0.09 m, and it tilts 26 degrees against horizontal direction. Cross-section on the horizontal plane becomes ellipse with major radius is 0.11 m. Figure 5 depicts spatial distribution of the magnetic field inside the channel along five straight reference lines parallel at 10 mm intervals as in right figures in Fig. 5 which shows mechanical image of the beam channel.

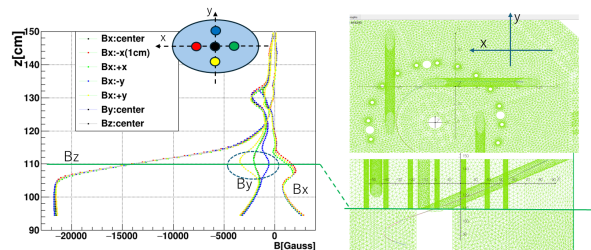


Figure 5: Magnetic field distribution inside the channel along five straight reference lines parallel at 10 mm intervals.

To understand how much affect on trajectories by such non-linear effects, several simple tracking are shown in Fig. 6. Initial beam positions at $z=1.48$ m are differ as in left side of fig 6, but momentum of each trajectory is same. Right side pictures in Fig. 6 give us how much linearity is conserved along the beam channel.

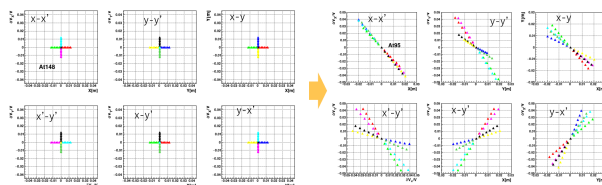


Figure 6: Left: initial positions of sample trajectories at the entrance of beam channel ($z=1.48$ m). Right: Sample beam positions at the exit of the beam channel ($z=1.10$ m).

Figure 7 depicts magnetic field of the first derivative distribution at the exit of the yoke channel ($z=0.11$ m). Black and pink dots are beam cross-section for type-A and type-B for comparison. To minimize non-linear effect especially at the exit of the channel, the beam should stay in the area of the smaller first derivative distribution.

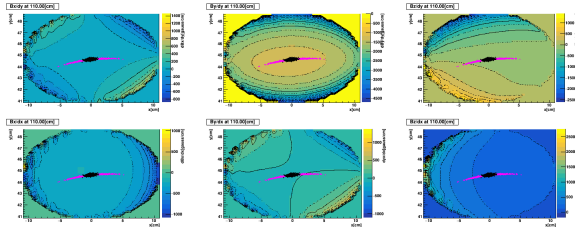


Figure 7: Beam shape at the exit of the yoke channel with magnetic field of the first derivative distribution.

Beam Shape at the Entrance of the Yoke Channel

In order to determine the specifications of the transport line upstream from the point of injection on the storage magnet ($z=1.45$ m, indicated as red star in Fig. 1), we present the results of finding the phase space using a reverse trajectory from $z=0.95$ m, indicated in yellow star in Fig. 1 or in Fig. 2.

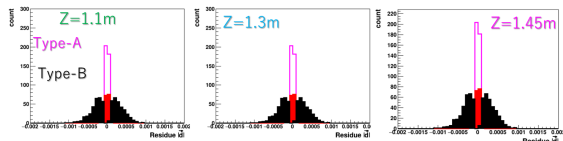


Figure 8: Same as Fig. 4 but different positions in the channel at $z=1.10$, 1.30 and 1.45 m.

Figure 8 presents the results of singular value decomposition of the phase space at several locations within the channel and evaluation of the validity of the X-Y coupling using the minimum value vector. Both agree with the index of $VBO < 0.05$ m, indicating that the phase space within the channel can also be adjusted by the correlation of the X-Y coupling.

ROTATING QUADS IN UPSTREAM TRANSPORT LINE

Figure 9 depicts current design of beam transport line [4] which satisfies X-Y correlation indicated in aqua-blue line in Fig. 10 by use of SAD. Basic parameters of two cases of seven rotating quadrupoles are summarised in Table 1. These two cases give the same transport matrix.

In order to shape a very flat beam as in Fig. 10 it is necessary to have a large Twiss parameter- β at the incident point. We are considering installing another rotating quadrupoles and/or rotating dipoles for beam shaping in the area that is currently preserve as free space.

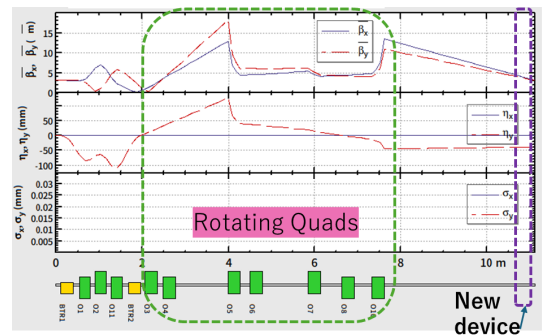


Figure 9: Picture of rotating quadrupole magnet and support system.

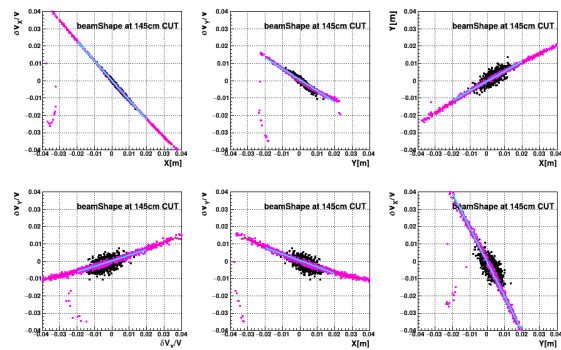


Figure 10: Phase space at $z=1.45$ m as pointed with red star in Fig. 1. The pink(black) colored distribution is type-A(type-B), which is traced back from Fig. 2. Aqua-blue solid lines are linear fit of pink colored distributions.

Table 1: Basic Parameters for Two Cases: Design-1 /-2

Quad ID	Integ. K [T]	Rot. angle [deg.]
Q3	-5.86 / 4.77	-30.6 / 45
Q4	1.07 / 0.08	-51.3 / 45
Q5	0.21 / 0.61	-61.6 / 60
Q6	0.19 / 0.018	-57.2 / -60
Q7	0.30 / 0.23	-61.1 / -60
Q8	-0.19 / -0.011	-36.8 / 45
Q9	-0.67 / 0.529	-58.2 / -60

SUMMARY AND NEXT

In this paper, required phase space at several points as in Fig. 1 are introduced. To accomplish requirements, non-linear effect in the beam channel of the yoke is studied and confirm less effect which allow us to control X-Y correlation along entire transport line including the channel. As a next step, for more precise and better tuning ability, a dedicated magnets called active shield multipole magnet will be required at the entrance and the exit of the beam channel of the storage magnet yoke. A prototype rotating quadrupole has been produced, and test bench works to measure attitude control accuracy and magnetic field are currently underway.

REFERENCES

- [1] M. Abe *et al.*, “A new approach for measuring the muon anomalous magnetic moment and electric dipole moment”, *Prog. Theor. Exp. Phys.*, vol. 2019, no. 5, May 2019. doi:10.1093/ptep/ptz030
- [2] H. Inuma *et al.*, “Three-dimensional spiral injection scheme for the g-2/EDM experiment at J-PARC”, *Nucl. Instrum. Methods Phys. Res., Sect. A*, vol. 832, pp. 51–62, Oct. 2016. doi:10.1016/j.nima.2016.05.126
- [3] H. Inuma *et al.*, “Precise control of a strong X-Y coupling beam transportation for J-PARC muon g-2/EDM experiment”, in *Proc. IPAC'23*, Venice, Italy, May 2023, pp. 304-307. doi:10.18429/JACoW-IPAC2023-MOPA110
- [4] H. Inuma *et al.*, “Design of a Strong X-Y Coupling Beam Transport Line for J-PARC Muon g-2/EDM Experiment”, *IEEE Trans. Appl. Supercond.*, vol. 32, no. 6, pp. 1–5, Sep. 2022. doi:10.1109/tasc.2022.3161889